



Journal Name

ARTICLE

Received 00th January 20xx,
Accepted 00th January 20xx

DOI: 10.1039/x0xx00000x

www.rsc.org/

Conformational Analysis of Enantiomerization Coupled to Internal Rotation in Triptycyl-*n*-helicenes

A. Carreras,^a L. Fuligni,^b P. Alemany,^b M. Llunell,^b J. M. Bofill,^c and W. Quapp^d

We present a computational study of a reduced potential energy surface (PES) to describe enantiomerization and internal rotation in three triptycyl-*n*-helicene molecules, centering the discussion on the issue of a proper reaction coordinate choice. To reflect the full symmetry of both strongly coupled enantiomerization and rotation processes, two non-fixed combinations of dihedral angles must be used, implying serious computational problems that required the development of a complex general algorithm. The characteristic points on each PES are analyzed, the intrinsic reaction coordinates calculated, and finally projected on the reduced PES. Unlike what was previously found for triptycyl-3-helicene, the surfaces for triptycyl-4-helicene and triptycyl-5-helicene contain valley-ridge-inflection (VRI) points. The reaction paths on the reduced surfaces are analyzed to understand the dynamical behaviour of these molecules and to evaluate the possibility of a molecule of this family exhibiting a Brownian ratchet behaviour.

Introduction

Motion at the micro and nanoscale has been studied intensively in the last decades^{1–6} and many achievements were obtained for micro and nano-devices whose motion depends on their shape, composition, and the power source that propels them. These

microscopic motors work all through a stimulus triggering a response on the device, allowing some kind of unidirectional motion. External stimuli can be as varied as a chemical substance reacting with one of such motors^{7–10} or the application of an external field used to power the device and control its motion^{11–14} (for example employing a magnetic material and an external electric or magnetic field). In some cases it is even possible to apply both mechanisms simultaneously to increase the overall control of motion.^{15–17} When reducing the device's dimensions up to a few nanometers, however, its motion follows a random path with a behaviour defined as Brownian motion. This kind of motion is also associated with a low Reynolds number, indicating that in these cases the motors are operating in a very viscous regime. In fact, in this regime, quantum phenomena associated to the confinement of electrons become more evident, causing a separation of the energy levels.

A specific kind of nano-devices are the so called molecular machines and motors, that is, single molecules able to perform a certain task through a stimulus responsive mechanism. Molecular machines are particularly interesting because their extreme miniaturization allows a minimization of friction due to interaction forces between the different parts of the device (van der Waals forces, local polarizations by induced dipoles, etc.). With respect to their macroscopic mechanical counterparts, the mechanical strength, that increases with the size of a system, is drastically reduced, achieving higher operational frequencies due to the increase in the resonance frequency as the size of the system is progressively reduced.^{18–20} The dynamic behaviour of these machines is quite different from that known for macroscopic analogues and much work is still needed in order to fully understand how molecular devices work and to suggest how to modify their design to increase their efficiency.

Concerning molecular motors, an interesting way to produce an overall unidirectional rotation motion may be to employ thermal energy, as in the so called “Brownian ratchets”.²¹ However, to obtain continuous unidirectional rotation, an additional necessary condition is that the chemical path corresponding to this unidirectional rotation should be also the lowest energy path on their potential energy surface (PES). In other words, the net forces acting on the molecule should always favour rotation in the desired direction.

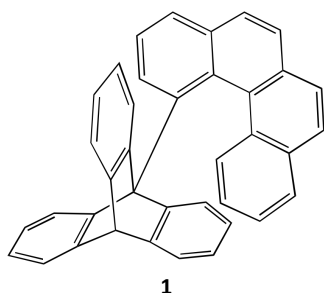
In this respect, Kelly and coworkers published several papers about a series of molecular compounds where they proposed that they should behave like molecular brakes or rotors.^{22–27} One of these molecules

^a Donostia International Physics Center (DIPC), Paseo Manuel de Lardizabal, 4, 20018 Donostia, Euskadi, Spain.

^b Departament de Ciència de Materials i Química Física & Institut de Química Teòrica i Computacional (IQTCUB). Universitat de Barcelona, Martí i Franquès 1, 08028 Barcelona, Spain.

^c Departament de Química Inorgànica i Orgànica & Institut de Química Teòrica i Computacional (IQTCUB). Universitat de Barcelona, Martí i Franquès 1, 08028 Barcelona, Spain.

^d Mathematisches Institut, Universität Leipzig, PF 100920, D-04009 Leipzig, Germany.



was assimilated to a ratchet, where the triptycyl part (shown in blue in Fig. 1) represents a dented disk with three teeth, while the helicene (shown in red in Fig. 1) would correspond to a deformable stiff pawl attached to the trypticyl group by a single C–C bond (in yellow in Fig. 1a) that functions as an axle.²³ Actually, the molecule represented in Fig. 1 is a simplified version of that synthesized by Kelly which contained a methyl group attached to the helicene, a detail that is not relevant for our discussion below.

According to ¹H NMR data, slow rotation of the triptycyl side is achieved at 160 °C if the helicene has four rings, while the triptycyl does not rotate if the helicene has only three rings.²³ Energy barriers deduced from experimental data corroborate this result, pointing towards a higher barrier for the 3–helicene case (~27 kcal mol⁻¹) with respect to that of the 4–helicene one (~25 kcal mol⁻¹). At first sight this may appear as a counterintuitive result because for a macroscopic machine, a longer “pawl” should imply more “friction” and so provide a higher energy barrier for the reaction. Although experimental data presented in the original paper²³ clearly discard the existence of unidirectional rotation, the potential energy profile shown in Ref. 23 for rotation around the axle appears to be strongly asymmetric, giving rise to the speculation of the possibility of unidirectional rotation in molecules containing 4–helicene. However, the sudden energy drop shown in figure 2 of Ref. 23 points clearly towards a computational artefact resulting from an insufficient mathematical representation of the system that is undergoing a complex stereodynamics.²⁸ As shown for the case of triptycyl–3–helicene, one single reaction coordinate is not enough to properly represent both the enantiomerization and rotation pathways that the molecule may simultaneously undergo. Since the interconversion between two enantiomeric minimum energy geometries of the molecule may follow two different chiral paths, one enantiomeric from the other one, these reactions proceed via a nonsynchronous narcissistic reaction path^{29,30} described by two reaction coordinates that change their sign because they must be antisymmetric with respect to the mirror plane of the reaction. From this it follows that at least two independent antisymmetric coordinates are needed to obtain a correct representation of the PES for the rotation / enantiomerization process in the triptycyl–3–helicene molecule and to project the intrinsic reaction coordinates (IRC) on it,^{28,30} while the use of a single coordinate describing just the internal rotation as in figure 2 of Ref. 23 is doomed to failure.

The conclusions of the analysis of the PES for the T3H molecule²⁸ show that the minimum energy paths for this molecule are narcissistic paths (NPs) that link two of the six isomeric

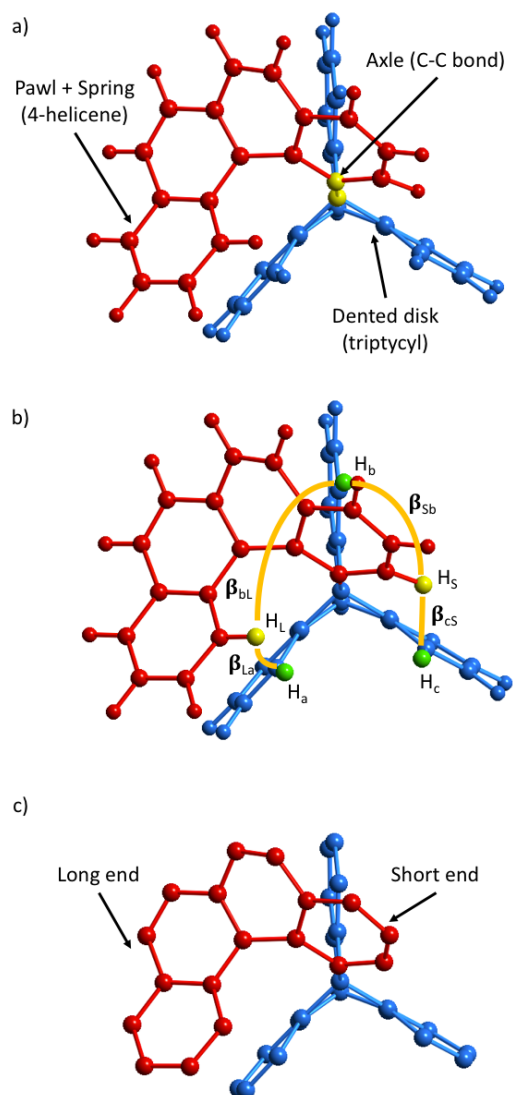


Fig. 1 a) One of the 6 isomeric minimum energy geometries of the triptycyl-4-helicene and its operational components as a molecular rotor. b) The hydrogen atoms chosen to define the dihedral angles for this geometry (green and orange atoms) and an indication of the angles themselves. c) Molecule carbon skeleton as used in PES maps to describe characteristic configurations.

minimum energy geometries, showing that enantiomerization is easier than rotation. This result is in good agreement with the experimental ¹H NMR data obtained by Kelly et al.²³ that are compatible either with a mixture of two helical enantiomers undergoing a rapid racemization or with an improbable case of a planar 3–helicene fragment without rotation.

Although our previous study presented in Ref. 28 shed some light in the subtleties of the dynamic behaviour of triptycyl-*n*-helicenes, there is still an important open question concerning the influence of the enantiomerization process in the overall dynamic behaviour of the T4H molecule that, counter intuitively, is found to

perform slow rotations. A first possible explanation was given by Kelly et al.²³ considering the strong repulsive interactions between the long end (Fig. 1c) of the helicene and the triptycyl blades to prevent the trapping of the helicene fragment in low energy configurations between two consecutive triptycyl blades.

The purpose of the present work is to better understand the stereodynamic behaviour of the T4H molecule, trying to unravel its working mechanism so that the same principles could be possibly extended to other molecular devices and nanomotors. For this reasons, we present a comparative analysis of the PESs for a set of TnH molecules where *n*, the length of the helicene fragment, changes from 3 to 5.

Theoretical Concepts and Procedure

A. Potential energy surface and reaction branching

It is well established that any molecular structure can be specified by its geometry, that is the stereo arrangement of its atoms, and its electronic state, which is associated to the wave function that describes the electronic distribution of the molecule. To each molecular structure we can then associate a specific energy that will depend on these parameters. For each electronic state, the 3*N* dimensional hyperspace that describes how the energy of the molecule changes as a function of the coordinates of the *N* nuclei forming the molecule is known as its potential energy surface (PES). The PES discussed in most theoretical calculations is the adiabatic PES, in which the Born-Oppenheimer approximation is used to solve the time independent Schrödinger equation. This approximation imposes a fixed position of the nuclei when calculating the electronic structure. In many instances, the full 3*N* dimensionality of the adiabatic PES can be reduced if one is only interested in the evolution of the molecule's energy for a specific transformation, for instance a chemical reaction, that can be described as a function of a reduced subset of the molecule's internal coordinates. The most typical case is to describe a chemical reaction by a potential energy curve, where the evolution of the energy along a path in the 3*N* space of molecular coordinates, the so-called reaction path (RP), is described by just a single parameter. Important concepts such as first order saddle point (SP) and transition state (TS), used in this work to characterize a RP are thoroughly discussed in Refs. 31-33.

Although the most commonly used strategy is just to use one internal coordinate (or a combination of them) to describe the RP, this approach is not always feasible since, in fact, sometimes it leads to an artificial discontinuous energy profile that does not describe the real structural transformation taking place at the molecular level. For instance, in the series of TnH molecules described here, rotation of the triptycyl blades around the central C-C bond can not be described by a single dihedral angle since a coordinate associated to the helicene torsion (and possible enantiomerization) is also implied in the conformational changes, so that both process are inevitably coupled and at least two

independent coordinates are needed to fully describe the dynamical behaviour of these molecules.

Two minima that are connected by the RP represent reactants and products of a reaction. From a mathematical point of view, the RP is conventionally defined as the mass-weighted steepest descent path from a TS. This last definition represents the so-called intrinsic reaction coordinate (IRC) of a reaction. The IRC is determined by a system of differential equations along the vector tangent to the curve that is the energy gradient of the PES. Since the gradient is zero only in stationary points, the IRC, and hence, the RP, is univocally defined connecting the TS and a minimum.^{32,33}

If, however, a branching of the reaction path occurs, the IRC is no longer a suitable model to describe a RP because the IRC cannot have bifurcations or branches other than at the SPs.³²⁻³⁵

Reaction path branching is associated with particular points of the PES that are independent from the definition of the curve and are usually associated to a symmetry breaking. Such points are known as valley ridge inflections (VRIs). A VRI point, by definition, is characterized by a zero eigenvalue of the Hessian matrix that corresponds to a zero-eigenvector which is orthogonal to the gradient.³⁵ From this definition VRIs are points where at least one main curvature of the hypersurface becomes zero orthogonally to the gradient and they are usually non-stationary points on the PES.^{32,35} VRIs are particularly interesting for reaction rate theory.³⁶ In fact, if the branching occurs after a transition state, the branching ratio of the reaction depends only on the nature of the PES and how it bifurcates. VRIs are not easily identifiable and many techniques such as the reduced gradient following or gradient extremals³²⁻³⁵ have been employed in the last decades to find them.

B. Narcissistic reactions

Narcissistic reactions and narcissistic paths (NPs) were first proposed and studied by Salem et al. in the '70.^{29,30} Among them we find most of the enantiomerization processes where reactants and products are not related by an improper rotation axis, as well as many automerization processes too. A reaction is defined as narcissistic if reactants and products are mirror images with respect to a fixed plane, and the mirror image of any point of the reaction path corresponds to a point in the "reverse" reaction path. In the first part of the definition, reactant and product images are defined with respect to a single space-fixed set of coordinate axes referred to the reaction mirror plane. Narcissistic reactions are equivalent to pure reflections with respect to this mirror plane as represented in Fig. 2 (see also figure 7 of Ref. 37). This plane, which is uniquely defined, depends however on the reaction process and it does not necessarily need to be a plane of symmetry for the starting configuration (either reactant or product). Notice that, as expected, the definition takes into account the invariance of the system under translations and rotations.²⁹ From these definitions it follows that each point in the RP of a narcissistic reaction must correspond to another point on the "reverse" RP with a geometry that is enantiomeric with respect to the mirror plane that characterizes the narcissistic reaction.

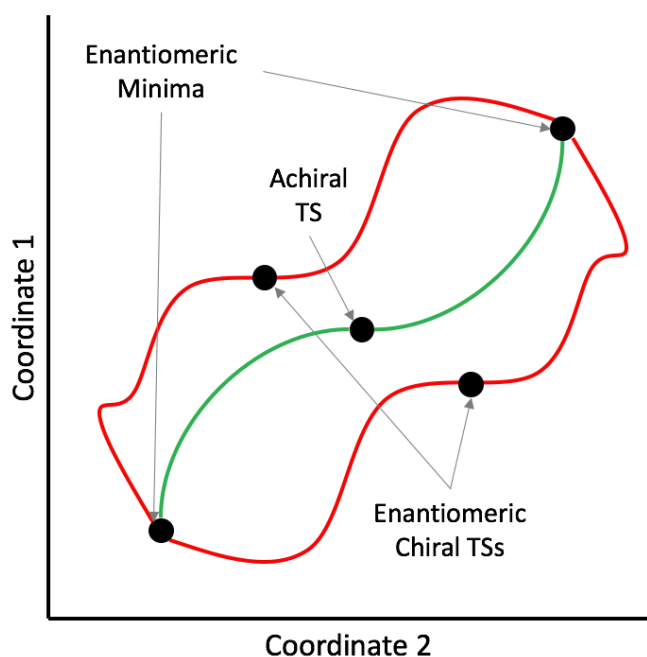


Fig. 2 Schematic representation of the projection of the interconversion path between two enantiomeric minima on a reduced PES. An achiral geometry is located in the middle point between the minima and its plane of symmetry acts as a mirror plane between any pair of enantiomeric conformations. On the PES, the corresponding point acts as an inversion center between any pair of energy points corresponding to enantiomeric chiral configurations. For this reason we will use indistinctly the term "mirror" to refer to both the actual symmetry plane for the achiral TS and to the inversion center on the PS.

Depending on the features of the PES, in some special cases NPs can be described by a single curve that crosses the mirror, located exactly at the middle point between reactants and products. At this precise point the system becomes achiral, and the mirror plane is a plane of symmetry (type I NPs, green curve in Fig. 2). In the other cases two distinct paths connect the reactant to the product and vice versa. They pass around the mirror without crossing each other and they terminate where the other "reflected" path begins. The overall result is two mirrored chiral paths (type II NPs, red curves in Fig. 2) with their respective enantiomeric transition states.

Type I NPs are characterized by a synchronism in the reaction, while in the second type there is an intrinsic non-synchronous behaviour. The reaction path type depends on how the molecular geometry changes during the reaction. In other words, to have a narcissistic reaction (that is pure reflection and not a simple rotation or translation) at least a coordinate among the system of coordinates chosen to characterize the reaction must change sign during the reaction (i.e. from a to $-a$) a situation that happens when the coordinates are antisymmetric with respect to the mirror.³⁰ If there is a single antisymmetric coordinate, the path crosses the mirror plane at the middle point of the path where the coordinate value equals zero, the reaction is type I and can be represented

with a line along the axis of the coordinate. If, instead, there are two antisymmetric coordinates, it is more convenient to employ a two-dimensional plot to represent changes in the two involved variables. If these two antisymmetric coordinates are strongly coupled and change in a synchronous manner then it is a type I NP. However, if there is a significant lag between the variation in the two coordinates and they change non-synchronously during a reaction, then it is a type II narcissistic reaction. In the extreme case, any chiral path can be divided into two segments: in the first one a coordinate changes while the other is left behind, while in the second one the latter coordinate catches up with respect to the former one. The opposite mechanism occurs in the other, enantiomeric, chiral path.

From the preceding discussion it is clear that the number of antisymmetric coordinates and how they are coupled play a major role on the type of a narcissistic reaction, determining the presence of an achiral transition state on the mirror plane (type I) or two distinct chiral transition states, one on each chiral path (type II). The behaviour of these antisymmetric coordinates in a narcissistic reaction is then the key element that determines the mechanistic behaviour of the reaction. The change in sign of at least one antisymmetric coordinate is a necessary characteristic of a narcissistic reaction and it can be employed to distinguish this reaction from an overall rotation, where the coordinates change from zero to zero and no antisymmetric coordinate changes sign.³⁰ In this respect, the choice of proper coordinates for the representation of the reaction course is a crucial issue.

C. Coordinate choice for TnH molecules

Following our previous work on the T3H case,²⁸ to study the internal rotation process in molecules of the TnH family we will use a two-dimensional reduced PES to properly describe the coupling of the purely rotational motion of the triptycyl rotor with that of enantiomerization of the helicene fragment. As found for the T3H molecule,²⁸ all these systems present a set of 6 minima, grouped in two sets with different handedness, namely, M and P, following the usual nomenclature for isolated helicenes. The 3 M (3 P) minima are equivalent structures related by rotation. On the other hand, any M minimum is related to two P minima by two mirrors, as any P minimum is related to two M minima. In the full PES (rotation from 0° to 360°) 6 mirror points will be found. The presence of these mirrors implies that any reaction path between minima must be a NP since they do not pass through a mirror since this would imply a very energetic achiral TS.

Since the reaction paths in these systems are NPs, at least one of the coordinates of the subspace used to construct the projected adiabatic 2-dimensional PES must remain antisymmetric with respect to all three planes of symmetry of the reaction path where the triptycyl fragment rotates around the single C–C bond. These planes of symmetry are each one of the mirror planes containing one of the three blades of the triptycyl rotor. Several dihedral angles defined by an atom on the helicene fragment, the two carbon atoms that form the axle, and an atom on the triptycyl

fragment are antisymmetric with respect to the plane defined by one of the triptycyl blades and may be used. Of all possible choices it appears to us more convenient to employ hydrogen atoms on the two fragments of the molecule to define these dihedral angles because they are less constrained than the carbon ones. Among these hydrogen atoms, the best choice on the triptycyl side are the three (H_A , H_B , H_C) hydrogen atoms oriented toward the helicene fragment as evidenced in Fig. 1b, one on each blade. For the helicene fragment, the hydrogen atoms that we use are at the opposite ends of the fragment: the first one at the "short" end and the other at the "long" end (Fig. 1c). This choice of atoms to define the dihedrals is applied for any molecule of the TnH family (each molecule of this family will be referred to by the label TnH, where n indicates the length of the helicene fragment, here $n = 3, 4, 5$). The three mirror planes used to characterize enantiomerizations along the triptycyl's rotation path correspond each to one of the three blades of the triptycyl fragment. As the helicene ends (short and long) move and pass over all three triptycyl blades in a full turn, the reference mirror plane changes and the dihedral angles that were antisymmetric with respect to the old mirror plane are not antisymmetric anymore. The chosen coordinates must, however, be antisymmetric with respect to all these planes, and this is achieved by using a non-fixed combination of the dihedral angles mentioned above. This combination changes along the reaction path according to the position of the helicene fragment with respect to the triptycyl blades (see Electronic Supplementary Information). In this way enantiomerization and rotation are represented correctly since the chosen combinations of dihedral angles are always antisymmetric with respect to the changing mirror plane. For a given position, the selected dihedral angles are indicated in Fig. 1b. There are two angles for each end of the helicene fragment with respect to the two nearest triptycyl blades: β_{sb} and β_{cs} for the short side, β_{la} and β_{bl} for the long one.

A full rotation of the triptycyl fragment accounts for three successive narcissistic reactions, so that these coordinates must be antisymmetric with respect to a different mirror plane for each transition between two minima. However, as mentioned above, it is more convenient, to employ a non-fixed combination of such angles to obtain a description for the whole reduced PES that properly reflects its full symmetry. The angles α_S and α_L used to construct the reduced PES are then two combinations of those dihedral angles: α_S involves two dihedrals defined using hydrogen atoms at the short (S) end of the helicene fragment, while α_L involves two analogous dihedrals for the long (L) end,

$$\alpha_S = 120^\circ \cdot n_S + \frac{\beta_{sb}}{\beta_{sb} + \beta_{cs}} \cdot 120^\circ \quad (1)$$

$$\alpha_L = 120^\circ \cdot n_L + \frac{\beta_{la}}{\beta_{la} + \beta_{bl}} \cdot 120^\circ \quad (2)$$

In eqns (1) and (2), β_{la} , β_{bl} , β_{sb} , β_{cs} are the dihedrals described in Fig. 1b, while n_S and n_L are integer values used to keep track of the degree of internal rotation when the ends of the helicene move with respect to a reference position in the triptycyl rotor

corresponding to the blade that contains the H_A hydrogen atom (see Fig. 1b). As long as n_S and n_L do not change, the two triptycyl blades closest to each end of the helicene will remain the same. Changing these values in eqn (1) or eqn (2) results in the rotation of the corresponding end of the helicene toward one of the contiguous sectors delimited by two consecutive triptycyl blades. If the n_X value increases, the X end of the helicene moves to the contiguous sector in a clockwise direction. If it decreases, the corresponding end of the helicene fragment will move counter-clockwise. For this reason, the values of n_S and n_L indicate also which dihedral angles are considered in each moment and in this way, which is the actual plane of symmetry that is being considered.

During a counter-clockwise rotation path starting with the structure depicted in Fig. 1b, when the H_L atom goes over H_a , dihedral β_{la} must equal 0° and α_L equals $120^\circ \cdot n_L$. If the rotation continues, then the H_L atom will be located between the H_a and H_c atoms. From that point onwards n_L changes to $n_L - 1$ and the β dihedral angles considered will be β_{al} and β_{lc} . This construction ensures the continuity and antisymmetric character of the considered α coordinates.

Although due to the presence of the helicene fragment the angles between planes containing two different triptycyl blades are strictly non-equivalent and somewhat different from the ideal 120° value, in the equation to determine the values for the α angles, β_{sb} and β_{la} (dihedral angles for the ends of the helicene fragment with respect to the closest counter-clockwise triptycyl blade), are normalized to 120° in order to keep the three-fold symmetry of the reduced PES.

To give a better description of the coupling between the internal rotation and the enantiomerization processes it is useful to define two new coordinates more directly associated with each of the two different processes.²⁸ We chose them so that one coordinate changes sign when moving from one structure to its enantiomer, while the other one changes from 0° to 360° when a full rotation has been completed. These new coordinates, related to the handedness (α_H) of the helicene fragment and to its rotation with respect to the triptycyl fragment (α_R) are obtained from linear combinations of the α_S and α_L angles defined previously, namely,

$$\alpha_R = \frac{\alpha_S + (\alpha_S - 180^\circ)}{2} \quad (3)$$

and

$$\alpha_H = \alpha_L - (\alpha_S - 180^\circ) \quad (4)$$

We used then these two coordinates, α_R and α_H , to obtain a two-dimensional reduced PES where α_R values are restricted between 0° and 360° , while α_H ones between -180° and 180° . Angle α_H is a parameter that can be used to easily distinguish between different enantiomers; it ranges between negative and positive values and changes sign during enantiomerizations because this coordinate is antisymmetric and it equals 0° for all the mirror points. When its value is not equal to 0° , then its sign indicates if the molecule is left- or right-handed. Out of the mirror planes, an α_H equals 0° does not

imply a non bended helicene fragment, since this angle is a measure of handedness just for the two helicene ends, not for the full fragment. But on the mirror points, the full molecule has no handedness because it has an achiral conformation. α_R represents the internal rotation performed by the triptycyl blade around the central C-C axle. Since the dihedral angles are normalized between 0° and 120° , an increase of 120° in α_R with respect to a given geometry means that the molecule has performed a partial rotation. This means that the ends of the helicene are in different positions and one blade of the triptycyl fragment closest to at least one of the helicene ends has changed. This implies that the calculation of the reduced PES can be restricted to values in the $0^\circ < \alpha_R \leq 120^\circ$ interval and then replicated: for angles between 120° and 360° each geometry corresponds to a geometry where the triptycyl fragment is rotated by 120° or 240° , with the same potential energy as the corresponding isomeric structure between 0° and 120° .

Results and Discussion

All the calculations of the examples presented and discussed in this section were performed using the AM1 molecular orbital model and the UHF wave function.³⁸ This semiempirical method is, in our opinion, sufficient for our purposes, because in this work our interest is focused on the global topological features of the PES and not in a detailed description of the geometry and the energy of each individual configuration. Moreover, the AM1 method has been shown to be adequate to study the enantiomerization of [n]helicene compounds.³⁹ The IRC path was located employing the algorithm of González and Schelegel⁴⁰ as implemented in the Gaussian⁴¹ and GAMESS⁴² codes. As explained in more detail in the supplementary material, the calculation of a reduced PES for the studied molecules can not be directly obtained using the standard optimization routines included in these programs, and an in-house code has been developed for this purpose. In order to have an idea of the huge computational task involved in producing one of the reduced PES plots shown in the next section, note that it is necessary to perform about 50000 geometry optimizations to obtain a sufficiently smooth surface interpolated from the potential energies calculated at a regular grid of points, an enormous computational task that can be only achieved at a rational cost using semiempirical quantum chemical methods.

A. The T3H Potential Energy Surface

For the reasons explained above, just a rhomboid portion of each PES needs to be calculated. In the previous study²⁸ of this molecule, the complete surface for T3H was calculated and it has been used to construct the PES shown in Fig. 3.

The IRCs computed and projected on this surface evidence the presence nonsynchronous NPs (NNPs) corresponding to two enantiomerizations: one has minima M_i and P_i , as reactant and product, respectively, while the other connects minima P_i and M_{i+1} . To achieve a rotation, that is for instance to move from minimum

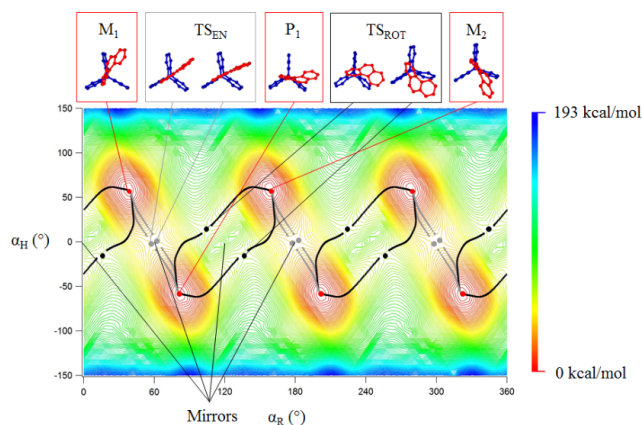


Fig. 3 Reduced PES for T3H represented as a contour map with the IRC projected on it. M_i and P_i correspond to the minimum energy isomers, while TS_{EN} and TS_{ROT} indicate the two TSs, respectively, for enantiomerization by transition of either the short or the long ends. The mirrors planes correspond actually to the inversion centers of the PES and are located between any pair of NPs.

M_i to M_{i+1} (or equivalently from P_i to P_{i+1}) the T3H molecule has to perform two consecutive enantiomerizations (for example, $M_i \rightarrow P_i \rightarrow M_{i+1}$) that present very different energy barriers (Table I). In the first one, for example from M_1 to P_1 , corresponding to the pass of the short end of the helicene over a triptycyl blade, the computed energy barrier is $14.8 \text{ kcal mol}^{-1}$. To achieve a rotation, this molecule has to perform a further enantiomerization, this time between P_1 and M_2 , where the long end of the helicene passes over another triptycyl blade. The computed energy barrier in this case is $29.0 \text{ kcal mol}^{-1}$. This confirms previous results^{24,28} about the presence of an energy barrier too high to achieve full rotation, producing a rapid enantiomerization that results in a racemic mixture. In other words, in the T3H molecule, to obtain an enantiomerization reaction only one end of the helicene has to get over a triptycyl blade, but to achieve a rotation, both ends of the helicene need to pass a blade in two successive enantiomerizations. Since one of these two enantiomerizations has a much higher barrier, we do not observe the rotation, but just the racemization process due to enantiomerization following back and forth the path with the lower of the two barriers.

The high energy barrier for the second enantiomerization process arises mainly due to the large torsion of the helicene fragment with respect to its minimum energy conformational structure that is needed before it can pass a blade avoiding highly repulsive triptycyl-helicene interactions. As it is evident in Fig. 3, the NNPs corresponding to these two processes are also very different. The pair of NNPs between M_1 and P_1 pass close to the reaction's mirror, where the achiral geometry is located, while the NNPs that connect P_1 and M_2 pass further away from their corresponding mirror. As Salem theorized,³⁰ this result is linked to the degree of synchronism of the reaction coordinates. These are much strongly coupled in the first enantiomerization, the one with a lower barrier, than in the second one.

Table I

| COMPUTED ENERGY BARRIERS AND EXPERIMENTAL RESULTS | | | | | |
|---|--|----------|---|--------------|----------|
| Molecule | Enantiomerization barriers (kcal mol ⁻¹) | | Rotation barriers (kcal mol ⁻¹) | | |
| | Previous | Computed | Previous | Experimental | Computed |
| T1H | -- | 3.8 | -- | -- | 3.8 |
| T2H | -- | 3.9 | -- | -- | 21.5 |
| T3H | 15.6 [28] | 14.8 | 27.0 [24] 27.4 [28] | >27 [24] | 29.0 |
| T4H | -- | 24.1 | 22.0 [24] | 24.5 [24] | 21.8 |
| T5H | -- | >33.4 | 16.0 [28] | -- | 16.2 |

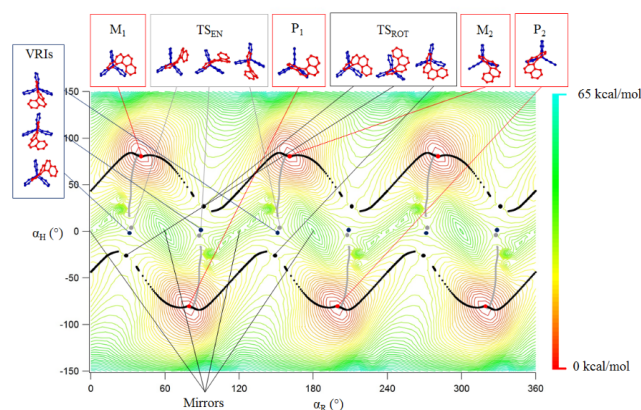


Fig. 4 Reduced PES for T4H represented as a contour map with the IRC projected on it. M_i and P_i are the minimum isomers. TS_{EN} and TS_{ROT} are the TS for the enantiomerization and rotation reactions, respectively. The mirrors are the centre of symmetry of the PES and the mirror of the NNP. VRIs indicate the estimated positions of the corresponding VRI points.

B. The T4H Potential Energy Surface

Despite the structural analogy between the two molecules, the reduced PES calculated for the T4H case, Fig. 4, has strikingly different features from that found for T3H. The reduced PES presents in this case branched RPs arising from branching in the complete surface. This feature is usually linked to a symmetry breaking of the orbitals of the molecular system and is directly correlated with the presence of VRI points on the PES. The branching results in a new RP, which does not exist on the T3H surface. Counterintuitively it allows for a pure rotation moving from a minimum P_i (or M_i) to one of the other nearby minima, $P_{i\pm 1}$ (or $M_{i\pm 1}$) without the necessity of involving intermediate enantiomerizations (crossing the $\alpha_H = 0$ line). The two NNPs, described above for the T3H molecule, are still present in this surface, but now each RP belonging to one NNP is merged with a RP of the other NNP. The energy barrier obtained in the enantiomerization path between P_i and M_i is 24.1 kcal mol⁻¹. However, due to branching and the presence of a VRI point this RP contains another SP that is the TS for pure rotation. The calculated energy barrier for this SP is 21.8 kcal mol⁻¹. This means that the pure rotation path is energetically favoured due to a lower energy barrier. Due to the symmetry of the PES, the enantiomerization between P_i and $M_{i\pm 1}$ appears to have the same features with two SPs and a VRI between them. Note also that, as a result of these features of the PES, the barrier for rotation in T4H (21.8 kcal mol⁻¹) is lower than that in T3H (29.0 kcal mol⁻¹, corresponding to the higher of the two necessary enantiomerization processes), an unexpected finding that is in good agreement with the experimental measurements obtained by Kelly et al.²³

Thus, for the T4H molecule, for a given minimum energy geometry, both enantiomerizations (for instance, P_1 to M_1 and P_1 to M_2) are possible and have the same energy barrier. Since there is a pure rotation RP for moving from M_i to $M_{i\pm 1}$ (or P_i to $P_{i\pm 1}$) with a

lower energy barrier than for the enantiomerization path, for a certain temperature range it should be even possible to observe free rotation in a non-racemic system.

C. The T5H Potential Energy Surface

As we can observe in the PES of T5H (Fig. 5), the direct rotation paths connecting M–M or P–P minima are still present for this molecule. So, pure rotation is also possible for T5H. We calculate its associated TS and its energy barrier to be 16.2 kcal mol⁻¹, even lower than for the T4H case. As shown in Table I, the computed rotation energy barrier is mainly correlated with the length of the helicene fragment. In that table the experimental and calculated barriers for rotation and enantiomerization for the T_nH molecules are reported. Although their full PESs have not been computed, the energy barriers have been calculated also for T1H and T2H molecules.

Exceptuating the first two T1H and T2H cases, which strictly speaking do not correspond to helicene fragments, the shorter the helicene, the higher the rotation energy barrier. This trend may be explained taking into account that for sterical reasons a longer helicene presents a flatter structure in the minimum energy geometry and, therefore, it must undergo less conformational changes to pass over any of the triptycyl blades. In fact, the energy barrier expresses the energy increment from the corresponding minimum energy and in a conformational study (no bonds broken or formed) energy variations are correlated only to structural changes.

In the region limited by the dashed red lines, the PES shown in Fig. 5 is not well defined since the proposed set of coordinates leads to a non univocal definition for the molecular geometry at each point. Crossing this region in a vertical direction the energy profile shows a large discontinuity. Even in the zones around the mirrors where the energy profile seems to be continuous, its derivative

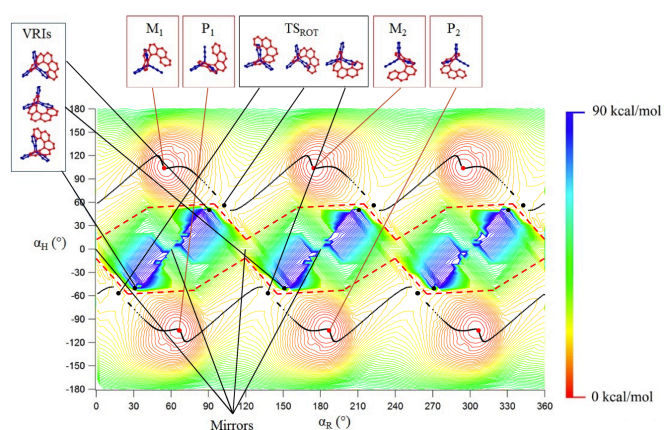


Fig. 5 Reduced PES for T5H represented as a contour map with the IRC projected on it. M_i and P_i are the minimum isomers. TS_{ROT} is the TS for the rotation reaction. VRIs indicate the estimated positions of the corresponding VRI points. The region limited by the dashed red lines the PES is not well defined.

shows a discontinuity. It indicates that two points very close to a mirror plane correspond to two enantiomeric geometries with the same energy, but far away of the very high energy achiral structure. This problem around the points corresponding to mirrors also happens in the two previous PES maps, but since the paths circumvent the mirror and do not pass through them, they do not pose any problem to the analysis presented above. Since the length of the helicene increases further in the T5H, a higher enantiomerization energy barrier is expected. In fact, in the reduced PES of T5H an extremely high energy zone emerges along the $\alpha_H = 0^\circ$ axis, which must be crossed by any possible enantiomerization path.

The computed PES seems to evidence the presence of another SP that could be associated with the enantiomerization RP because it is located on the α_R axis providing an apparent energy barrier of $33.4 \text{ kcal mol}^{-1}$. This point ($60^\circ, 0^\circ$) also corresponds to the mirror of the reaction but from the computation of the PES, the obtained point does not correspond to an achiral geometry since any plane of symmetry implies a vertical flat helicene and, therefore, a geometry far from any local minimum. This non-unequivocal correspondence between energy and geometry at these points has already been observed in the previous T3H study. If any RP passes too close to one of the points where the mirror planes are projected on the reduced PES it cannot be well represented using these reaction coordinates. This is what seems to happen with the enantiomerization RP in the T5H molecule. In this SP, the molecule structure corresponds to a point that belongs to the border which separates the valley and the ridge regions of the PES.

The presence of this point indicates the presence of a branching on the full PES of T5H and the existence of VRI points. The VRIs are estimated to be very close to the TS_{ROT} . The presence of a VRI point in the T5H PES could have different implications than in the T4H

molecule because it seems to be located closer to TS_{ROT} and the presumed RP for enantiomerization probably connects two of these symmetric TSs. It is, however, necessary to do a more refined study of the PES for structures around the projected mirrors to draw any definitive conclusions.

On the other hand, it has to be mentioned that the two ends of the helicene fragment pass simultaneously over a triptycyl blade in T4H and T5H molecules. This is simply associated to the length of the helicene that, as the length increases, when it assumes a completely planar structure, it is closer to a perfect circle. As a consequence, the two ends are close to a triptycyl blade both in a rotation and in an enantiomerization reaction. So, for T4H and T5H each transition of the long end over the blade implies also a possible transition of the short side of the helicene fragment. The increase in length allows also a higher degree of conformational freedom for the helicene allowing a minimum energy with a spiral-like shape. In the T3H case the pure rotation would require a very high energy relative to the minimum energy configuration. In T4H and T5H the blades of the triptycyl would act as constraints to keep the helicene in its spiral-like conformation. In this situation structural changes to the shape of the helicene require a high energy due to the confinement between the blades of the triptycyl, limiting the possible conformational changes of the helicene while the molecule rotates.

In summary, the T5H PES contains a rotation path as shown in Fig. 5, but it does not seem to present an enantiomerization path. Looking at the energy surface, this hypothetical path would imply a very high energy. Although we have widely searched for a transition state in the region between M and P enantiomers, it has not been possible to locate any, leading us to conclude that most probably the enantiomerization path does not exist for this structure.

Conclusions

The computed barriers that we have obtained (Fig. 6) for the series of TnH molecules are compatible with previous experimental data and calculations.^{24,28} A deeper analysis of the PES shows that the RPs for T4H and T5H evidence the existence of a pure internal rotation path that is not present in the T3H molecule, leading to an explanation of the counterintuitive experimental finding that rotation is easier in the systems with longer helicene fragments. We have also shown that the PESs calculated for T4H and T5H contain VRI points whose positions have been roughly estimated. Starting from the VRI point of the T4H system, the RP connecting TS_{EN} and TS_{ROT} was computed. The presence of a VRI indicates that in those points of the PES the molecules could both perform rotation and enantiomerization, making these two reactions correlated one with the other.

Supposing that thermal fluctuations from the environment are strong enough, pure rotation is impossible for T3H but it is feasible in the T4H molecules due to a decrease in the rotation barrier and the presence of a VRI along the enantiomerization path. However, if the thermal energy is not too high, rotation seems to be the only

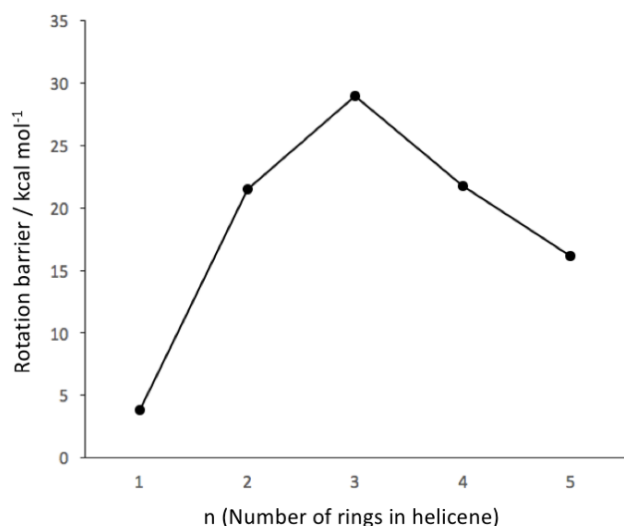


Fig. 6 Variation of the rotation barrier in the triptycyl-*n*-helicene systems when increasing the number of rings in the helicene pawl.

possible RP for the T5H. This makes T5H a better candidate for designing a Brownian ratchet, in front of the two other molecules. From the observed correlation between energy barriers and the length of the helicene, it is possible to speculate that the T6H molecule, could be even a better candidate, since a higher enantiomerization barrier and a smaller rotation barrier are expected in this case.

It must be underlined, however, that these molecules behave as rotors, not as motors, since they may rotate indistinctively in both clockwise and counter-clockwise directions. In this sense, the T_nH molecules do not seem to be accurately represented by a dented disk, an axle and a pawl as suggested in Ref. 23. The triptycyl fragment is more akin to a flexible disk with three empty “sectors” and the helicene can be considered as a pawl only if its length is at least equal to four.

If we analyse the set of PESs obtained for the different T_nHs we can conclude that the topography of each PES is much more important than the actual values of the rotation barriers to predict a possible ratchet behaviour. In a more detailed way, due to the relative low enantiomerization barriers in T3H and T4H any conformational path and the corresponding mirror image are equally accessible from any initial conformation with a total energy (kinetic plus potential) of the order of the highest energy barrier. For this reason these two systems do not present ratchet behaviour since any rotation in a direction can be counteracted through an identical path. Since in the T5H system the enantiomerization is not possible, the clockwise rotation path is not identical to the anticlockwise path although these two paths share the same energy barrier. Since the barriers are the same in both directions, clockwise and anticlockwise evolutions are possible, but the differences in the reaction path shape could lead to different probabilities for each direction. Thus this system is not a perfect ratchet, but it could

evolve preferentially in one direction (molecule evolves as a Brownian ratchet).²¹

Summarizing our findings we think that the stereodynamical behaviour of the T5H molecule should be further studied to confirm the existence of a preferential unidirectional motion. This study should, however, not be limited to the energy barriers since, as found in the present study, the topology of the PES and the detailed dynamical behaviour are predicted to be crucial to evaluate both thermodynamic and kinetic effects for this system.

Acknowledgements

Financial support from the Spanish Ministerio de Economía y Competitividad, Projects CTQ2015-64579-C3-3-P and CTQ2016-76423-P, Spanish Structures of Excellence María de Maeztu program through grant MDM-2017-0767, and from the Generalitat de Catalunya, Departament d'Empresa i Coneixement, Projects 2017 SGR 348 and 2017 SGR 1289, is acknowledged.

Notes and references

- S. J. Ebbens and J. R. Howse, *Soft Matter*, 2010, **6**, 726.
- C. Bechinger, R. Di Leonardo, H. Löwen, Ch. Reichhardt, G. Volpe and G. Volpe, *Rev. Mod. Phys.*, 2016, **88**, 045006(50).
- W. Wang, T. Y. Chiang, D. Velegol and T. E. Mallouk, *J. Am. Chem. Soc.*, 2013, **135**, 10557.
- V. Yadav, W. Duan, P. J. Butler and A. Sen, *Annu. Rev. Biophys.*, 2015, **44**, 77.
- W. Wang, W. Duan, S. Ahmed, A. Sen and T. E. Mallouk, *Acc. Chem. Res.*, 2015, **48**, 1938.
- A. Solovev, S. Sanchez and O. G. Schmidt, *Nanoscale*, 2013, **5**, 1284.
- S. Sanchez, L. Soler and J. Katuri, *Angew. Chem. Int. Ed.*, 2015, **54**, 1414.
- D. Vilela, J. Parmar, Y. Zeng, Y. Zhao and S. Sanchez, *Nano Letters*, 2016, **16**, 2860.
- W. Duan, R. Liu and A. Sen, *J. Am. Chem. Soc.*, 2013, **135**, 1280.
- W. Gao, M. D'Agostino, V. Garcia-Gradilla, J. Orozco and J. Wang, *Small*, 2012, **9**, 467.
- V. Garcia-Gradilla, J. Orozco, S. Sattayasamitsathit, F. Soto, F. Kuralay, A. Pourazary, A. Katzenberg, W. Gao, Y. Shen and J. Wang, *ACS Nano*, 2013, **7**, 9232.
- A. Ghost and P. Fischer, *Nano Lett.*, 2009, **9**, 2243.
- L. Zhang, K. E. Peyer and B. J. Nelson, *Lab on a Chip*, 2010, **10**, 2203.
- P. Calvo-Marzal, S. Sattayasamitsathit, S. Balasubramanian, J. R. Windmiller, C. Dao and J. Wang, *Chem. Commun.*, 2010, **46**, 1623.
- W. Wang, W. Duan, Z. Zhang, M. Sun, A. Sen and T. E. Mallouk, *Chem. Commun.*, 2015, **51**, 1020.
- X. Ma and S. Sanchez, *Chem. Commun.*, 2015, **51**, 5467.
- J. G. Gibbs and Y. Zhao, *Small*, 2010, **6**, 1656.
- C. Bustamante, D. Keller and G. Oster, *Acc. Chem. Res.*, 2001, **34**, 412.
- E. R. Kay, D. A. Leigh and F. Zerbetto, *Angew. Chem. Int. Ed.*, 2006, **46**, 72.
- G. S. Kottas, L. I. Clarke, D. Horinek and J. Michl, *Chem. Rev.*, 2005, **105**, 1281.
- P. Reimann, *Phys. Rep.*, 2002, **361**, 57

- 22 T. R. Kelly, M. C. Bowyer, K. V. Bhaskar, D. Bebbington, A. Garcia, F. Lang, M. H. Kim and M. P. Jette, *J. Am. Chem. Soc.*, 1994, **116**, 3657.
- 23 T. R. Kelly, I. Tellitu and J. P. Sestelo, *Angew. Chem. Int. Ed. Engl.*, 1997, **36**, 1866.
- 24 T. R. Kelly, I. Tellitu and J. P. Sestelo, *J. Org. Chem.*, 1998, **63**, 3655.
- 25 T. R. Kelly, H. De Silva and R. Silva, *Nature*, 1999, **401**, 150.
- 26 T. R. Kelly, *Acc. Chem. Res.*, 2001, **34**, 514.
- 27 T. R. Kelly, X. Cai, F. Damkaci, S. B. Panicker, B. Tu, S. M. Bushell, I. Cornella, M. J. Piggott, R. Salives, M. Cavero, Y. Zhao and S. Jasmin, *J. Am. Chem. Soc.*, 2007, **129**, 376.
- 28 M. Llunell, P. Alemany and J. M. Bofill, *ChemPhysChem*, 2008, **9**, 1117.
- 29 L. Salem, J. Durup, G. Bergeron, D. Cazes, X. Chapuisat and H. Kagan, *J. Am. Chem. Soc.*, 1970, **92**, 4472.
- 30 L. Salem, *Acc. Chem. Res.*, 1971, **4**, 322.
- 31 H. B. Schlegel, *Computational Molecular Science*, 2011, **1**, 790.
- 32 W. Quapp, M. Hirsch and D. Heidrich, *Theor. Chem. Acc.*, 2004, **112**, 40; J. M. Bofill and W. Quapp, *J. Chem. Phys.*, 2011, **134**, 074101.
- 33 W. Quapp and B. Schmidt, *Theor. Chem. Acc.*, 2011, **128**, 47; J. M. Bofill and W. Quapp, *Theor. Chem. Acc.*, 2016, **135**, 11.
- 34 W. Quapp, M. Hirsch and D. Heidrich, *Theor. Chem. Acc.*, 1998, **100**, 285.
- 35 W. Quapp, *J. Mol. Struct.*, 2004, **695–696**, 95; J. M. Bofill and W. Quapp, *J. Math. Chem.*, 2013, **51**, 1099.
- 36 W. Quapp and J. M. Bofill, *J. Comput. Chem.*, 2016, **37**, 2467
- 37 M. Llunell, P. Alemany and J. M. Bofill, *Theor. Chem. Acc.*, 2008, **121**, 279.
- 38 M. J. S. Dewar, E. G. Zoebisch, E. F. Healy and J. J. P. Stewart, *J. Am. Chem. Soc.*, 1985, **107**, 3902.
- 39 S. Grimme, S. D. Peyerimhoff, *Chem. Phys.*, 1996, 204, 411; R. H. Janke, G. Haufe, E. U. Würthwein, J. H. Borkent, *J. Am. Chem. Soc.*, 1996, **118**, 6031.
- 40 C. González, H. B. Schlegel, *J. Chem. Phys.*, 1989, **90**, 2154
- 41 M. J. Frisch et al., "Gaussian 09, Revision B. 01," Gaussian Inc., Wallingford, CT, 2004.
- 42 M. W. Schmidt, K. K. Baldrige, J. A. Boatz, S. T. Elbert, M. S. Gordon, J. H. Jensen, S. Koseki, N. Matsunaga, K. A. Nguyen, S. J. Su, T. L. Windus, M. Dupuis and J. A. Montgomery, *J. Comput. Chem.*, 1993, **14**, 1347].